The Cryosphere Discuss., 8, 307–335, 2014
www.the-cryosphere-discuss.net/8/307/2014/
doi:10.5194/tcd-8-307-2014

The Cryosphere Discussions | Open Access

Fabric measurement along the NEEM ice core, Greenland, and comparison with GRIP and NGRIP ice cores

M. Montagnat[1,2], N. Azuma[3], D. Dahl-Jensen[4], J. Eichler[5,6], S. Fujita[7], F. Gillet-Chaulet[1,2], S. Kipfstuhl[5], D. Samyn[3], A. Svensson[4], and I. Weikusat[5]

[1]CNRS, LGGE, UMR5183, 38041 Grenoble, France
[2]Univ. Grenoble Alpes, LGGE, 38041 Grenoble, France
[3]Department of Mechanical Engineering, Nagaoka University of Technology, 1603-1 Kamitomioka, Nagaoka 940-2188, Niigata, Japan
[4]Niels Bohr Institute, Ice and Climate Research, University of Copenhagen, Juliane Maries Vej 30, 2100 Copenhagen, Denmark
[5]Alfred Wegener Institute for Polar and Marine Research, Columbusstrasse, 27568 Bremerhaven, Germany
[6]Fachbereich Physik, Freie Universitat Berlin, Arnimallee 14, 14195 Berlin, Germany
[7]National Institute of Polar Research, Research Organization of Information and Systems (ROIS), Midori-chou 10-3, Tachikawa, Tokyo, 190-8518 Japan

Received: 4 November 2013 – Accepted: 12 December 2013 – Published: 14 January 2014

Correspondence to: M. Montagnat (montagnat@lgge.obs.ujf-grenoble.fr)

Published by Copernicus Publications on behalf of the European Geosciences Union.

Abstract

Fabric (distribution of crystallographic orientations) profile along the full NEEM ice core, Greenland, is presented in this work. Data were measured in the field by an Automatic Ice Texture Analyzer every 10 m, from 33 m down to 2461 m depth. The fabric evolves from a slightly anisotropic fabric at the top, toward a strong single maximum at about 2300 m, which is typical of a deformation pattern mostly driven by uniaxial compression and simple shearing. A sharp increase in the fabric strengthening is observed at the Holocene to Wisconsin climatic transition. A similar strengthening, toward an anisotropic single maximum-type fabric, has been observed in several ice cores from Greenland and Antarctica, and can be attributed to a positive feedback between changes in ice viscosity at the climatic transition, and the impact of a shear component of stress. Centimeter scale abrupt texture (fabric and microstructure) variations are observed in the bottom part of the core. Their positions are in good agreement with the folding hypothesis used for a climatic reconstruction by Dahl-Jensen et al. (2013). Comparison is made to two others ice cores drilled along the same ridge; the GRIP ice core drilled at the summit of the ice sheet, and the NorthGRIP ice core, drilled 325 km to the NNW of the summit along the ridge, and 365 km upstream from NEEM. The fabric profile clearly reflects the increase in shear deformation when moving NW along the ridge from GRIP to NorthGRIP and NEEM. The difference in fabric profiles between NEEM and NorthGRIP also evidences a stronger lateral extension associated with a sharper ridge at NorthGRIP.

1 Introduction

Crystal preferred orientation, or fabric, analyses along ice cores drilled in polar ice sheets are highly necessary to access conditions and perturbations of deformation along ice cores. While grain size evolution is traditionally associated with climatic changes (Duval and Lorius, 1980; Durand et al., 2006b), the fabric evolution depends

TCD
8, 307–335, 2014

primarily on the dominant stress system, and the fabric strength is often related to the cumulative strain (Alley, 1988; Budd and Jacka, 1989).

Under deformation conditions typical for ice cores drilled on ice divides, the *c*-axis distribution of the ice crystals rotate towards a compression axis, perpendicular to a shear direction, and away from a tension axis (Gow and Williamson, 1976; Alley, 1988; Paterson, 1994). The fabric profile along a core is then a good candidate to evaluate the nature of the flow and to extract irregularities in the deformation history if present. In the specific case of a perfect dome, the ice deforms solely by uni-axial compression along the vertical direction (Alley, 1988). This is qualitatively confirmed by the fabrics measured along cores such as those of Greenland GRIP (Thorsteinsson et al., 1997), and Antarctic Dome Fuji (Azuma et al., 1999), EPICA Dome C (Wang et al., 2003; Durand et al., 2009), and Talos Dome (Montagnat et al., 2012) which are all located close to topographic domes. At NorthGRIP, Greenland, (Wang et al., 2002) and Vostok, (Lipenkov et al., 1989) and EDML, (Bargmann et al., 2011), Antarctica, a vertical girdle fabric is observed, which characterizes regions with a strong component of horizontal tension.

The fabric depth profile along ice cores generally follows a continuous trend. Departure from this trend can be attributed to dynamic recrystallization processes such as observed at the deepest part of the GRIP ice core (Thorsteinsson et al., 1997), and the GISP2 ice core (Gow et al., 1997), as well as at various depths in the Siple Dome ice core, Antarctica (Diprinzio et al., 2005), for instance. They may also be attributed to a positive feedback between variations in ice viscosity, which in turn are related to variations in dust content, and the impact of a shear stress component that is increasing with depth. This was observed at EPICA Dome C at 1750 m depth during termination 2 (Durand et al., 2007) and at the Wisconsin–Holocene transition at Talos Dome (Montagnat et al., 2012).

A 2540 m long ice core was drilled at NEEM, Greenland, during field seasons 2008 to 2012 (77.45° N, 51.06° W, surface elevation 2450 m, mean annual temperature −29 °C, accumulation of 0.22 m ice equivalent per year) (Dahl-Jensen et al., 2013). The drill site

TCD
8, 307–335, 2014

is located downstream on the ice ridge that runs north-northwest from the summit of the Greenland ice sheet where the GRIP core was extracted (Dansgaard et al., 1993), see Fig. 1. Along this ridge, one can also find the NorthGRIP ice core drilling site, 325 km to the NW of GRIP, and 365 km upstream from NEEM along the ridge towards Camp Century (Dahl-Jensen et al., 2002).

The NEEM drilling project was an international effort with 14 participating nations, with the main purpose to retrieve a continuous record of the whole Eemian interglacial (130–115 ka BP) (Buchardt and Dahl-Jensen, 2008). Indeed, ice from this period was found in the central Greenland ice cores (GRIP, GISP2 and NorthGRIP) but the records were too strongly disturbed, or too "short in time", to provide accurate climatic data from this period (Chappellaz et al., 1997; Cuffey, 2004).

The upper 1419 m of the NEEM ice core covers the current interglacial, the Holocene, and the glacial ice is found below down to 2206.7 m depth. Below this, the ice is disturbed and folded to some degree, but the Eemian record could be reconstructed from folded ice using globally homogeneous parameters known from other dated Greenland and Antarctic ice-core records (Dahl-Jensen et al., 2013).

The present work provides the fabric (crystal preferred orientation) data obtained at a relatively high resolution along the core (every 10 or 20 m). Section 2 will present the technical aspects of the measurements, and in Sect. 3 the results are presented. The discussion part, Sect. 4, will provide analyses of the results, and in particular, of the comparisons with GRIP and NorthGRIP ice cores.

2 Fabric measurements

The NEEM fabric data were obtained in the field, at the NEEM camp, during field seasons 2009 to 2011, from 33 m to 2461 m depth at a 10 m resolution. First, vertical thin ice core sections were produced directly from the extracted cores, except for the brittle ice zone that was drilled in 2009 but studied at the NEEM site in 2010. The brittle ice zone, extending from about 600 m to 1300 m depth, corresponds to ice highly affected structurally by the pressure from air bubbles that have not yet turned into chlathrates (Lipenkov, 2000; Kipfstuhl et al., 2001). A one year period is considered necessary to relax these constrains enough for ice to be processed.

The raw fabric data were obtained using two Automatic Ice Texture Analyzers (AITA) (Russell-Head and Wilson, 2001) of similar versions. The AITA provides c-axis orientations from thin sections of dimensions up to 12 cm × 12 cm at a resolution of 43 µm length for the older version (season 2009), and of 20 µm length for the more recent one (season 2010).

Orientation measurements are provided together with a quality factor that enables the elimination of sample areas of too high uncertainty, such as grain boundaries (Peternell et al., 2011). A threshold value for this quality factor was chosen at 70 % for all the thin sections studied.

The c-axis orientation $\mathbf{c}^k$ is defined by two angles: the co-latitude $\theta_k \in [0,\pi/2]$ (or tilt angle) and the longitude $\varphi_k \in [0,2\pi]$ given in the local reference frame, $\mathbf{R}$, with the third axis perpendicular to the thin section plan. The expression of $\mathbf{c}^k$ in this reference frame is:

$$\mathbf{c}^k = (\cos\varphi_k \sin\theta_k, \sin\varphi_k \sin\theta_k, \cos\theta_k) \qquad (1)$$

The orientation data are further represented in pole figures which are stereographic projections of the c-axis distributions.

The second-order orientation tensor $\mathbf{a}^{(2)}$ is used to characterize the c-axis orientation distribution (Wallbrecher, 1986; Thorsteinsson et al., 1997; Durand et al., 2006a). $\mathbf{a}^{(2)}$ is defined as:

$$\mathbf{a}^{(2)} = (1/N_\mathrm{p}) \sum_{k=1}^{N_\mathrm{p}} \mathbf{c}^k \otimes \mathbf{c}^k \qquad (2)$$

where $\mathbf{c}^k$ is given by Eq. (1), and N_p is the total number of pixels over which the $\mathbf{c}^k$ values are obtained for a given sample (thin section). Since the $\mathbf{c}^k$ values are obtained

TCD
8, 307–335, 2014

at a pixel size, the definition of $\mathbf{a}^{(2)}$ given by Eq. (2) implicitely takes into account the area of grains.

By construction, $\mathbf{a}^{(2)}$ is symmetric and there exists a symmetry reference frame, $\mathbf{R}^{\mathrm{sym}}$ (or principal reference frame), in which $\mathbf{a}^{(2)}$ is diagonal. Let $a_i^{(2)}$ (i=1,2,3) denote the three corresponding eigenvalues and $\mathbf{e}_i$ (i=1,2,3) the associated eigenvectors (the three base vectors of $\mathbf{R}^{\mathrm{sym}}$). The eigenvalues of $\mathbf{a}^{(2)}$ can be seen as the lengths of the axes of the ellipsoid that best fits the density distribution of grain orientations. The eigenvectors give the directions of the axes of the ellipsoid.

The three eigenvalues $a_1^{(2)}$, $a_2^{(2)}$ and $a_3^{(2)}$ follow the relations:

$$a_1^{(2)} + a_2^{(2)} + a_3^{(2)} = 1 \quad (3)$$

$$0 \leq a_3^{(2)} \leq a_2^{(2)} \leq a_1^{(2)} \leq 1 \quad (4)$$

For an isotropic fabric, $a_1^{(2)} = a_2^{(2)} = a_3^{(2)} = 1/3$, and when the fabric is transversely isotropic, two of the eigenvalues are equal:

$$a_2^{(2)} \approx a_3^{(2)} < 1/3 \text{ for a single-maximum fabric,} \quad (5)$$

$$a_1^{(2)} \approx a_2^{(2)} > 1/3 \text{ for a girdle fabric}$$

From a similar treatment of fabric data obtained along the Talos Dome ice core (Antarctica), Montagnat et al. (2012) showed that the standard deviation of the fabric data (eigenvalues of $\mathbf{a}^{(2)}$), associated with the analyzer measurement by itself, is very small. In particular, it is negligible compared to that induced by a sampling on a limited number of grains. This last standard deviation was estimated by Durand et al. (2006a) using a 3-D-Pott model to evaluate the influence of the under-sampling of a sample of 10 000 grains of the same size, on the evaluation of the orientation tensor eigenvalues. They obtained a relation between the standard deviation, the number of grains in the thin section, N_{g}, and the eigenvalue, Eq. (6). The same relation applies for the other two eigenvalues.

$$\sigma(a_i) = \left[-1.64 \times (a_1^{(2)})^2 + 1.86 \times a_1^{(2)} - 0.14\right] \times N_g^{-1/2}. \quad (6)$$

Although the grain size evolution along the NEEM core is not presented here, a few grain size data were measured and used to provide the standard deviation of the eigenvalues (Eq. 6) presented in the Fig. 2.

In order to evaluate the depth variability of the measurement at the local scale, fabric data were measured continuously along a few 55 cm long core sections, similarly to the approach of Svensson et al. (2003). At several depths along the core, this variability is taken into account by showing the eigenvalue data corresponding to every thin section that the 55 cm samples are composed of.

3 Results

3.1 Fabric evolution with depth

Figure 2 presents the fabric profile as a function of depth, using the three eigenvalues of the orientation tensor $\mathbf{a}^{(2)}$, together with the δ^{18}O record of NorthGRIP transferred to the NEEM depth scale using Rasmussen et al. (2013) chronology. This record can be used as a climate proxy as it is known to show the same climate variability as that of NEEM (the NEEM δ^{18}O record is not available yet). The error bars correspond to the standard deviation due to the limited number of grains on the thin section, as explain in Sect. 2. The largest error bars are encountered at depths where grain size is large compared to the thin section dimensions. For these depths, fabric data do not really have a true statistical meaning because of the low number of grains in the thin section. The lowest error bars are encountered in the upper part of the core (≈ first 200 m), where the grains are the smallest. The variability at a depth resolution higher than the thin section size is not considered as a measurement error (see Sect. 3.3).

TCD
8, 307–335, 2014

Figure 3 presents a few examples of microstructures and fabrics as pole figures at various depths along the core.

3.2 Comparison with the GRIP and NorthGRIP ice cores

Figures 4 and 5 show the fabric profile measured along the NEEM ice core compared respectively to that of the GRIP ice core (Thorsteinsson et al., 1997; Svensson et al., 2009) and of the NorthGRIP ice core (Wang et al., 2002; Svensson et al., 2009). The GRIP ice core was drilled at the present-day summit of the ice sheet, NorthGRIP ice core was drilled about 325 km away along the NNW ridge, and the NEEM ice core, located 365 km further, is close to a divergence departure point of the ridge line (Fig. 1). The main characteristics for the three coring sites are given in Table 1. The fabric is mainly related to the stress state and its intensity depends on the strain history. Therefore, the interpretation of the fabric differences between the cores requires estimates of the strain-rate histories experienced by the ice. Here we provide estimates of the actual strain-rates at the core locations as a function of depth. A rough first estimate of the mean vertical strain-rate D_{zz} can be obtained from the ratio between the annual ice accumulation a and the ice thickness H given in Table 1. This ratio is of similar order of magnitude at the three sites, between 6 and $9 \times 10^{-5}\,\mathrm{yr}^{-1}$. Furthermore, surface vertical strain-rates have been measured directly using a phase sensitive radar system near the GRIP and NEEM sites by Gillet-Chaulet et al. (2011), average values are $9.5 \times 10^{-5}\,\mathrm{yr}^{-1}$ and $11.5 \times 10^{-5}\,\mathrm{yr}^{-1}$ respectively. Hvidberg and Keller (2002) used surface velocity measurements in the NorthGRIP area to calculate surface strain rate in the direction transverse to the ice-divide ridge and obtained $7.4 \times 10^{-5}\,\mathrm{yr}^{-1}$. In Fig. 6 we assume that the vertical strain-rate along the cores follow a Dansgaard–Johnsen profile (Dansgaard and Johnsen, 1969), with a constant value of $10 \pm 1 \times 10^{-5}\,\mathrm{yr}^{-1}$ in the upper 2/3 of the ice thickness and then a linear decrease to 0. The vertical shear stress along the cores S_{xz}, in a local reference frame where x is aligned with the surface slope direction, is estimated using the shallow ice approximation (Greve and Blatter, 2009):

$$S_{xz} = \rho g z \mathrm{d}s/\mathrm{d}x, \tag{7}$$

with ρ being the ice density, g the standard gravity and z the depth from the surface. Surface slope $\mathrm{d}s/\mathrm{d}x$ is given in Table 1. The shear strain-rate D_{xz} is then estimated using Glen's flow law with a stress exponent $n = 3$ (Cuffey and Paterson, 2010)

$$D_{xz} = A(T) S_{xz}^3 \tag{8}$$

The rate parameter $A(T)$ depends on temperature T following a Arrhenius law. Estimates of the shear strain-rate along each core, assuming an uncertainty on the surface slope of $\pm 0.2\,\mathrm{m\,km^{-1}}$, are shown in Fig. 6. These estimates of the strain-rates along the cores do not take into account possible effects of the ice mechanical anisotropy induced by the fabric development or change in viscosity related with impurity content. Furthermore, the ice in the cores may have been deposited few kilometers to tens of kilometers upstream of the core locations, especially for NorthGRIP and NEEM (Dahl-Jensen et al., 2013), and then may have experienced a more complex strain-rate history than what is reflected by our estimates.

3.3 High resolution depth variability in the fabric data

High resolution depth variability in the fabric parameter at the mm-to-cm scale was observed at several depths along the NEEM core, from continuous measurements along 55 cm core sections. Although a specific study on this topic is scheduled, we thought it would be interesting to provide some basic observations.

Figure 7 shows examples of this high resolution variability measured at various depths along the core. For this measurement, the fabric eigenvalues were extracted on 5 or 6 thin sections contiguous along the 55 cm core section. Each data point in Fig. 7 is the average $a_1^{(2)}$ over these thin sections, and the error bar therefore represents the variability span in 10 cm resolution over the 55 cm depth interval.

TCD
8, 307–335, 2014
Fabric measurement along the NEEM ice core, Greenland
M. Montagnat et al.

The 55 cm samples do not cover equally long time periods at different depths of the core, which may explain part of the lower variability of the glacial samples that cover longer time periods.

3.4 Disturbed layers in the deepest part of the core

Dahl-Jensen et al. (2013) reconstructed the stratigraphy of the bottom part of the NEEM core from obviously folded ice layers. Stratigraphic disruptions were identified from discontinuities of the $\delta^{18}O_{ice}$ isotope and gas record measured in ice at several depths: 2209.60 m, 2262.15 m, 2364.45 m and 2432.19 m. These discontinuities were confirmed by N_2O, $\delta^{15}N$ and total air content measurements in the ice below 2200 m depth.

The existence of disturbed layers is also confirmed in high-resolution fabric and microstructure data. Figure 8 represents the NEEM stable water isotope record with emphasis on the discontinuities, together with microstructures and fabric pole figures from around these discontinuities. Figure 8 reveals a transition from "regular" grain size and "single maximum type" fabric to large grain size and multi-clustered fabric between 2008 and 2014 m depth, just in the vicinity of the $\delta^{18}O_{ice}$ discontinuity. Similar transitions were found between 2258 m and 2263 m, and between 2362.9 m and 2363 m depth, where the discontinuity can be captured within a single 10 cm thin section! Data measured at 2214 m depth is very similar to that measured at 2263 m, and measurement at 2258 m is very close to what is observed at 2362 m depth (with a slight tilt in the fabric which could correspond to a tilt introduced during sample preparation).

4 Discussion

The fabric profile along the NEEM ice core presents the classical feature of a progressive c-axis orientation strengthening with depth toward a single maximum. This feature is typical of a deformation pattern mostly driven by vertical compression and simple shearing that is observed in many ice cores retrieved from ice divides, such as GRIP, EPICA-Dome C, Talos Dome ice cores.

The initial fabric measured in the firn (from 33 m depth downwards) is not isotropic. This observation supports those from the EPICA Dome C ice core (Durand et al., 2009), the GRIP and NGRIP ice cores (Svensson et al., 2009) and the Talos Dome ice core (Montagnat et al., 2012), and contradicts the results obtained by Lomonaco et al. (2011) from sparse fabric measurements performed in the top 120 m of a firn core drilled at Summit, with the Electron Backscattering technique. The slightly clustered fabrics measured in the NEEM firn, which can not be explained by the level of strain reached at these depths (Montagnat et al., 2012), may be associated with fabric evolution mechanisms that could occur during firnification, in the upper hundred meter of the ice sheet. Further studies of fabric evolution in snow and firn are therefore necessary to better understand these observations (Riche et al., 2012).

Similar to the observations made along most of the deep Greenland and Antarctic ice cores, the c-axis orientation strengthening along the NEEM core is far from being monotonous. Indeed, a sharp increase in the strengthening rate is concomitant with the climatic transition between the Holocene and the Wisconsin periods. This transition is also characterized by a strong variation in the dust content, as observed along various Greenland ice cores (Steffensen et al., 2008). Therefore, following (Paterson, 1991) we could attribute the change in strengthening rate to some feedback between changes in ice viscosity from Winsconsin to Holocene ice, and the impact of a shear component of stress. The influence of a non negligible shear component of stress is necessary to explain the strong c-axis clustering observed in the range 1800 to 2000 m depth (Azuma and Higashi, 1985; Paterson, 1991; Alley, 1992; Thorsteinsson et al., 1997).

We can now compare three Greenland ice cores located along the same ridge, departing from a dome configuration at the summit of the ice sheet (Summit), Fig. 1. The fabric profile along the GRIP ice core is the most monotonous (Fig. 4), with no obvious abrupt changes at the onset of the Holocene, although a strong variation in the grain size evolution was measured at this transition (Thorsteinsson et al., 1997). GRIP is

TCD
8, 307–335, 2014

located near the dome where uniaxial compression is expected (vertical compression and uniform extension in the horizontal direction). This is mainly confirmed by the fabric profiles at GRIP where $a_2^{(2)} \approx a_3^{(2)} < a_1^{(2)}$. At a perfect ice divide, the dominant mode of deformation is believed to be pure shear, i.e., vertical compression accompanied by lateral extension (Paterson, 1994). Thorsteinsson et al. (1997) observed the effect of simple shear deformation between 2850 m and 2950 m depth where the fabric also becomes highly clustered. These highly clustered fabrics alternate with more open ones from about 2800 m depth, that appears together with a grain size increase explained by the influence of dynamic recrystallization mechanisms (Thorsteinsson et al., 1997).

The location along a ridge can induce an evolution of the fabric toward a girdle type, which characterizes pure shear deformation with an asymmetry of the horizontal extension. Along the NorthGRIP ice core, a strong vertical girdle pattern is evidenced by the increase of the $a_2^{(2)}$ eigenvalue compared to $a_3^{(2)}$, from 500 m depth down to about 2500 m. Below this depth, the fabric clusters with a change in the fabric strengthening rate (Fig. 5). This depth is much below the Wisconcin–Holocene transition, and the change is less abrupt than at NEEM.

A vertical girdle pattern is also observed along the NEEM core but less pronounced, and only down to the Wisconcin–Holocene transition. The asymmetry of the lateral extension is clearly lower at the NEEM site compared to NorthGRIP, where the ridge is sharper (Fig. 1). A sharp ridge inducing a strong asymmetry of the horizontal strain-rate components is also observed for the similar girdle-type fabrics for the EPICA-Dronning Maud Land ice core, Antarctica (Bargmann et al., 2011; Faria et al., 2014).

According to our estimates (Fig. 6) vertical compression dominates over vertical shear for at least the upper 1/3 to 2/3 part of the ice sheet. The estimated depth where shear strain-rate becomes dominant over vertical strain-rate is higher for NEEM than for NorthGRIP, in turn higher than the one for GRIP. These transition depths are in good agreement with the estimated depth of shear dominated fabric along the three cores.

The GRIP, NGRIP, and NEEM ice cores were drilled with a major objective of retrieving climatic information from the last interglacial period, the Eemien (between 130 000

TCD
8, 307–335, 2014

and 115 000 yr ago), when average temperature was five degrees warmer than today (Andersen et al., 2004). Stratigraphic disturbance in the bottom of the GRIP ice core prevented the core from revealing climatic information from this period of time (Chappellaz et al., 1997; Suwa et al., 2006). Layering in the deepest 10 % of the core was shown to be inclined by about 20° and discontinuous layering as well as small scale folds were observed (Alley et al., 1995). The NorthGRIP core proved to be located on a zone of high heat flow from the underlying crust (Dahl-Jensen et al., 2003). This heat melted the basal ice, eliminating the oldest ice layers, and only the latter few millennia of the Eemian could be retrieved (Cuffey, 2004). The high melting at the bottom of the NorthGRIP core significantly reduced the thinning of deep ice layers, allowing an annual resolution of the glacial-onset record (Svensson et al., 2011).

Fabric and microstructure signals in the bottom part of the NEEM core present a high variability (Sect. 3.4), in the area where clear evidence of folding was given by Dahl-Jensen et al. (2013). The abrupt variations in the microstructure and fabric signals are in agreement with the stratigraphical reconstruction performed by Dahl-Jensen et al. (2013). Nevertheless, the abrupt transition observed in texture between 2329.4 m and 2329.8 m depth does not correspond to any discontinuities in the stable isotope signal. Another scale of inhomogeneities must therefore exists within the layering induced by small scale folds. Such a folding configuration, which is typically observed at the base of glaciers and ice sheets where temperature and/or stress gradients are increased (Gow and Williamson, 1976; Herron and Langway, 1982; Budd and Jacka, 1989; Thorsteinsson et al., 1997; Samyn et al., 2008) has been observed at the base of the GRIP ice core, but not at the base of the NorthGRIP core. The comparison between the three cores therefore highlights the influence of the basal temperature and the shear component of stress on the thinning and the folding of the bottom layers.

TCD
8, 307–335, 2014

5 Conclusions

This paper presents the overall features of the fabric data measured in the field, every 10 m along the NEEM ice core, Greenland. The main observations are the following:

i. Similar to what was observed along other deep ice cores, the initial fabric, measured from 33 m depth downward, is not isotropic and may therefore be associated with fabric evolution during firnification.

ii. Down to about 1500 m depth, the fabric evolves toward a single maximum, with a slight girdle tendency. This is coherent with the position along a ridge, characterized by a vertical compression and a slight asymmetry in the horizontal extension.

iii. A sharp fabric strengthening is measured at the Holocene–Wisconsin transition, with a maximum reached at about 1800 m depth, and maintained down to 2300 m depth. Explanation may come from a feedback between ice viscosity changes around the climatic transition, and the impact of shear on the ice flow, as evidenced by Paterson (1991).

iv. Deeper in the ice core, the local variations of fabric and grain size support the folding hypothesis of Dahl-Jensen et al. (2013) and the suggested layering reconstruction.

v. A first-order comparison was made with the other two deep ice cores drilled along the same ridge, namely GRIP and NorthGRIP. This comparison evidences the increasing impact of shearing along the ridge, supported by the evaluation of the relative shear component of the strain-rate at the three sites. The higher impact of lateral extension along the NorthGRIP core coincides well with a sharper ridge at this site compared to NEEM. This comparison could be useful for further ice flow modeling along the ridge from GRIP to NEEM and onwards to Camp Century.

Acknowledgements. This work is a contribution to the NEEM ice core project, that is directed and organized by the Centre of Ice and Climate at the Niels Bohr Institute and US NSF, Office of Polar Programs. It is supported by funding agencies and institutions in Belgium (FNRS-CFB and FWO), Canada (NRCan/GSC), China (CAS), Denmark (FIST), France (IPEV, CNRS/INSU, CEA and ANR), Germany (AWI), Iceland (RannIs), Japan (NIPR), South Korea (KOPRI), the Netherlands (NWO/ALW), Sweden (VR), Switzerland (SNF), the UK (NERC) and the USA (US NSF, Office of Polar Programs) and the EU Seventh Framework programmes Past4Future and WaterundertheIce. D.S. is currently funded by the Japanese Society for the Promotion of Science, and was supported by a "Ymer-80 stipender för polarforskning" (Sweden) during his stay at NEEM.

The publication of this article is financed by CNRS-INSU.

References

Alley, R. B.: Fabrics in polar ice sheets – development and prediction, Science, 240, 493–495, 1988. 310

Alley, R. B.: Flow-law hypotheses for ice-sheet modeling, J. Glaciol., 38, 245–255, 1992. 318

Alley, R. B., Gow, A. J., Johnsen, S. J., Kipfstuhl, J., Meese, D. A., and Thorsteinsson, T.: Comparison of deep ice cores, Nature, 373, p. 393, doi:10.1038/373393b0, 1995. 320

Andersen, K., Azuma, N., Barnola, J.-M., et al.: High resolution record of Northern Hemisphere climate extending into the last interglacial period, Nature, 431, 147–151, 2004. 320

Azuma, N. and Higashi, A.: Formation processes of ice fabric pattern in ice sheets, Ann. Glaciol., 6, 130–134, 1985. 318

Azuma, N., Wang, Y., Mori, K., Narita, H., Hondoh, T., Shoji, H., and Watanabe, O.: Textures and fabrics in the Dome F (Antarctica) ice core, Ann. Glaciol., 29, 163–168, 1999. 310

Bamber, J. L., Griggs, J. A., Hurkmans, R. T. W. L., Dowdeswell, J. A., Gogineni, S. P., Howat, I., Mouginot, J., Paden, J., Palmer, S., Rignot, E., and Steinhage, D.: A new bed elevation dataset for Greenland, The Cryosphere, 7, 499–510, doi:10.5194/tc-7-499-2013, 2013. 328

Title Page
Abstract | Introduction
Conclusions | References
Tables | Figures
◀| |▶
◀ ▶
Back | Close
Full Screen / Esc
Printer-friendly Version
Interactive Discussion

Bargmann, S., Seddik, H., and Greve, R.: Computational modeling of flow-induced anisotropy of polar ice for the EDML deep drilling site, Antarctica: the effect of rotation recrystallization and grain boundary migration, Int. J. Numer. Anal. Met., 36, 892–917, doi:10.1002/nag.1034, 2011. 310, 319

Buchardt, S. L. and Dahl-Jensen, D.: At what depth is the Eemian layer expected to be found at NEEM?, Ann. Glaciol., 48, 100–102, doi:10.3189/172756408784700617, 2008. 311

Budd, W. and Jacka, T.: A review of ice rheology for ice sheet modelling, Cold Reg. Sci. Technol., 16, 107–144, 1989. 310, 320

Chappellaz, J., Blunier, T., Kints, S., Dallenbach, A., Barnola, J.-M., Schwander, J., Raynaud, D., and Stauffer, B.: Changes in the atmospheric CH_4 gradient between Greenland and Antarctica during the Holocene, J. Geophys. Res.-Atmos., 102, 15987–15997, doi:10.1029/97JD01017, 1997. 311, 320

Cuffey, K. M.: Palaeoclimate: into an ice age, Nature, 431, 133–134, 2004. 311, 320

Cuffey, K. M. and Paterson, W. S. B.: The Physics of Glaciers, 4th edn., Academic, Amsterdam, 2010. 316

Dahl-Jensen, D., Albert, M. R., Aldahan, A., et al.: Eemian interglacial reconstructed from a Greenland folded ice core, Nature, 493, 489–493, 2013. 309, 310, 311, 316, 317, 320, 321, 329, 335

Dahl-Jensen, D., Gundestrup, N., Miller, H., Watanabe, O., Johnsen, S. J., Steffensen, J. P., Clausen, H. B., Svensson, A., and Larsen, L. B.: The NorthGRIP deep drilling programme., Ann. Glaciol., 35, 1–4, 2002. 311

Dahl-Jensen, D., Gundestrup, N., Gorgineni, S. P., and Miller, H.: Basal melt at NorthGRIP modeled from borehole, ice-core and radio-echo sounder observations., Ann. Glaciol., 37, 207–212, 2003. 320

Dansgaard, W. and Johnsen, S. J.: A flow model and a time scale for the ice core from Camp Century, Greenland, J. Glaciol., 8, 215–223, 1969. 315

Dansgaard, W., Johnsen, S. J., Clausen, H. B., Dahl-Jensen, D., Gundestrup, N. S., Hammer, C. U., Hvidberg, C. S., Steffensen, J. P., Sveinbjörnsdottir, A. E., Jouzel, J., and Bond, G.: Evidence for general instability of past climate from a 250 kyr ice-core record, Nature, 364, 218–220, 1993. 311

Diprinzio, C. L., Wilen, L. A., Alley, R. B., Fitzpatrick, J. J., Spencer, M. K., and Gow, A. J.: Fabric and texture at Siple Dome, Antarctica, J. Glaciol., 51, 281–290, 2005. 310

Durand, G., Gagliardini, O., Thorsteinsson, T., Svensson, A., Kipfstuhl, J., and Dahl-Jensen, D.: Ice microstructure and fabric: an up to date approach to measure textures, J. Glaciol., 52, 619–630, 2006a. 312, 313
Durand, G., Weiss, J., Lipenkov, V., Barnola, J., Krinner, G., Parrenin, F., Delmonte, B., Ritz, C., Duval, P., Röthlisberger, R., and Bigler, M.: Effect of impurities on grain growth in cold ice sheets, J. Geophys. Res., 111, F01015, doi:10.1029/2005JF000320, 2006b. 309
Durand, G., Gillet-Chaulet, F., Svensson, A., Gagliardini, O., Kipfstuhl, S., Meyssonnier, J., Parrenin, F., Duval, P., and Dahl-Jensen, D.: Change in ice rheology during climate variations – implications for ice flow modelling and dating of the EPICA Dome C core, Clim. Past, 3, 155–167, doi:10.5194/cp-3-155-2007, 2007. 310
Durand, G., Svensson, A., Persson, A., Gagliardini, O., Gillet-Chaulet, F., Sjolte, J., Montagnat, M., and Dahl-Jensen, D.: Evolution of the texture along the EPICA Dome C ice core, Supp. Issue Low Temperature Science, 68, 91–106, 2009. 310, 318
Duval, P. and Lorius, C.: Crystal size and climatic record down to the last ice age from Antarctic ice, Earth Planet. Sc. Lett., 48, 59–64, 1980. 309
Faria, S. H., Weikusat, C., and Azuma, N.: The microstructure of polar ice – Part 1: Highlights from ice core research, J. Struct. Geol., in press, 2014. 319
Gillet-Chaulet, F., Hindmarsh, R. C. A., Corr, H. F. J., King, E. C., and Jenkins, A.: In-situ quantification of ice rheology and direct measurement of the Raymond Effect at Summit, Greenland using a phase-sensitive radar, Geophys. Res. Lett., 38, doi:10.1029/2011GL049843, 2011. 315
Gow, A. J. and Williamson, T. C.: Rheological implications of the internal structure and crystal fabrics of the West Antarctic ice sheet as revealed by deep core drilling at Byrd Station, Geol. Soc. Am. Bull., 87, 1665–1677, 1976. 310, 320
Gow, A. J., Meese, D. A., Alley, R. B., Fitzpatrick, J. J., Anandakrishnan, S., Woods, G. A., and Elder, B. C.: Physical and structural properties of the Greenland Ice Sheet Project 2 ice core: a review, J. Geophys. Res.-Oceans, 102, 26559–26575, doi:10.1029/97JC00165, 1997. 310
Greve, R. and Blatter, H.: Dynamics of Ice Sheets and Glaciers, Springer, Berlin/Heidelberg, 2009. 316
Herron, S. L. and Langway, C. C. J.: A comparison of ice fabrics and textures at Camp Century, Greenland and Bird Station, Antarctica, Ann. Glaciol., 3, 118–124, 1982. 320

Hvidberg, C. S., Keller, K. and Gundestrup, N. S.: Mass balance and ice movement along the north-northwest ridge of the Greenland ice sheet at NorthGRIP, Ann. Glaciol., 35, 521–526, 2002. 315

Kipfstuhl, S., Pauer, F., Kuhs, W. F., and Shoji, H.: Air bubbles and Clathrate hydrates in the transition zone of the NGRIP Deep Ice Core, Geophys. Res. Lett., 28, 591–594, doi:10.1029/1999GL006094, 2001. 312

Lipenkov, V.: Air bubbles and air-hydrate crystals in the Vostok ice core, in: Physics of Ice Core Records, edited by: Hondoh, T., Hokkaido University Press, Sapporo Japan, 327–358, 2000. 312

Lipenkov, V. Y., Barkov, N. I., Duval, P., and Pimienta, P.: Crystalline texture of the 2083 m ice core at Vostok Station, Antarctica, J. Glaciol., 35, 392–398, 1989. 310

Lomonaco, R., Albert, M., and Baker, I.: Microstructural evolution of fine-grained layers through the firn column at Summit, Greenland, J. Glaciol., 57, 755–762, 2011. 318

Montagnat, M., Buiron, D., Arnaud, L., Broquet, A., Schlitz, P., Jacob, R., and Kipfstuhl, S.: Measurements and numerical simulation of fabric evolution along the Talos Dome ice core, Antarctica, Earth Planet. Sc. Lett., 357–358, 168–178, doi:10.1016/j.epsl.2012.09.025, 2012. 310, 313, 318

Paterson, W. S. B.: Why ice-age ice is sometimes soft, Cold Reg. Sci. Technol., 20, 75–98, 1991. 318, 321

Paterson, W. S. B.: The Physics of Glaciers, Pergamon, Oxford, 1994. 310, 319

Peternell, M., Russell-Head, D., and Wilson, C.: A technique for recording polycrystalline structure and orientation during in situ deformation cycles of rock analogues using an automated fabric analyser, J. Microsc.-Oxford, 242, 181–188, 2011. 312

Rasmussen, S. O., Abbott, P. M., Blunier, T., Bourne, A. J., Brook, E., Buchardt, S. L., Buizert, C., Chappellaz, J., Clausen, H. B., Cook, E., Dahl-Jensen, D., Davies, S. M., Guillevic, M., Kipfstuhl, S., Laepple, T., Seierstad, I. K., Severinghaus, J. P., Steffensen, J. P., Stowasser, C., Svensson, A., Vallelonga, P., Vinther, B. M., Wilhelms, F., and Winstrup, M.: A first chronology for the North Greenland Eemian Ice Drilling (NEEM) ice core, Clim. Past, 9, 2713–2730, doi:10.5194/cp-9-2713-2013, 2013. 314, 329

Riche, F., Schneebeli, M., and Tschanz, S.: Design-based stereology to quantify structural properties of artificial and natural snow using thin sections, Cold Reg. Sci. Technol., 79–80, 67–74, doi:10.1016/j.coldregions.2012.03.008, 2012. 318

Russell-Head, D. S. and Wilson, C. J. L.: Automated fabric analyser system for quartz and ice, J. Glaciol., 24, 117–130, 2001. 312
Samyn, D., Svensson, A., and Fitzsimons, S. J.: Dynamic implications of discontinuous recrystallization in cold basal ice: Taylor Glacier, Antarctica, J. Geophys. Res.-Earth, 113, F03S90, doi:10.1029/2006JF000600, 2008. 320
Steffensen, J. P., Andersen, K. K., Bigler, M., Clausen, H. B., Dahl-Jensen, D., Fischer, H., Goto-Azuma, K., Hansson, M., Johnsen, S. J., Jouzel, J., Masson-Delmotte, V., Popp, T., Rasmussen, S. O., Röthlisberger, R., Ruth, U., Stauffer, B., Siggaard-Andersen, M.-L., Sveinbjörnsdóttir, Á. E., Svensson, A., and White, J. W. C.: High-resolution Greenland Ice Core data show abrupt climate change happens in few years, Science, 321, 680–684, doi:10.1126/science.1157707, 2008. 318
Suwa, M., von Fischer, J. C., Bender, M. L., Landais, A., and Brook, E. J.: Chronology reconstruction for the disturbed bottom section of the GISP2 and the GRIP ice cores: implications for Termination II in Greenland, J. Geophys. Res.-Atmos, 111, D02101, doi:10.1029/2005JD006032, 2006. 320
Svensson, A., Baadsager, P., Persson, A., Hvidberg, C. S., and Siggaard-Andersen, M. L.: Seasonal variability in ice crystal properties at NorthGRIP: a case study around 301 m depth, Ann. Glaciol., 37, 119–122, 2003. 314
Svensson, A., Durand, G., Mathiesen, J., and Persson, A., and Dahl-Jensen, D.: Texture of the Upper 1000 m in the GRIP and NorthGRIP Ice Cores, Supp. Issue Low Temperature Science, 68, 107–113, 2009. 315, 318, 331, 332
Svensson, A., Bigler, M., Kettner, E., Dahl-Jensen, D., Johnsen, S., Kipfstuhl, S., Nielsen, M., and Steffensen, J. P.: Annual layering in the NGRIP ice core during the Eemian, Clim. Past, 7, 1427–1437, doi:10.5194/cp-7-1427-2011, 2011. 320
Thorsteinsson, T., Kipfstuhl, J., and Miller, H.: Textures and fabrics in the GRIP ice core, J. Geophys. Res., 102, 26583–26600, 1997. 310, 312, 315, 318, 319, 320, 331
Wallbrecher, E.: Graphische, rechnerische und statistische Verfahren, in: Tektonische und gefügeanalytische Arbeitsweisen, Enke, Stuttgart, 244 pp., 1986. 312
Wang, Y., Thorsteinsson, T., Kipfsuhl, J., Miller, H., Dahl-Jensen, D., and Shoji, H.: A vertical girdle fabric in the NGRIP deep ice core, North Greenland, Ann. Glaciol., 35, 515–520, 2002. 310, 315, 332
Wang, Y., Kipfstuhl, S., and Azuma, N.: Ice fabrics study in the upper 1500 m of the Dome C deep ice core, East Antarctica, Ann. Glaciol., 37, 97–104, 2003. 310

TCD
8, 307–335, 2014

Fabric measurement along the NEEM ice core, Greenland

M. Montagnat et al.

Table 1. Ice thickness (H), annual accumulation (a), average annual temperature (T_{yr}), ratio a/H and surface slope magnitude (ds/dx) in GRIP, NorthGRIP and NEEM ice cores (references are given in the text).

	H m	a ice eq. m yr^{-1}	T_{yr} °C	a/H $10^{-5} yr^{-1}$	ds/dx m km^{-1}
GRIP	3027	0.24	−32	7.9	0.53
NGRIP	3085	0.19	−32.5	6.1	0.90
NEEM	2540	0.22	−29	8.7	1.83

TCD
8, 307–335, 2014

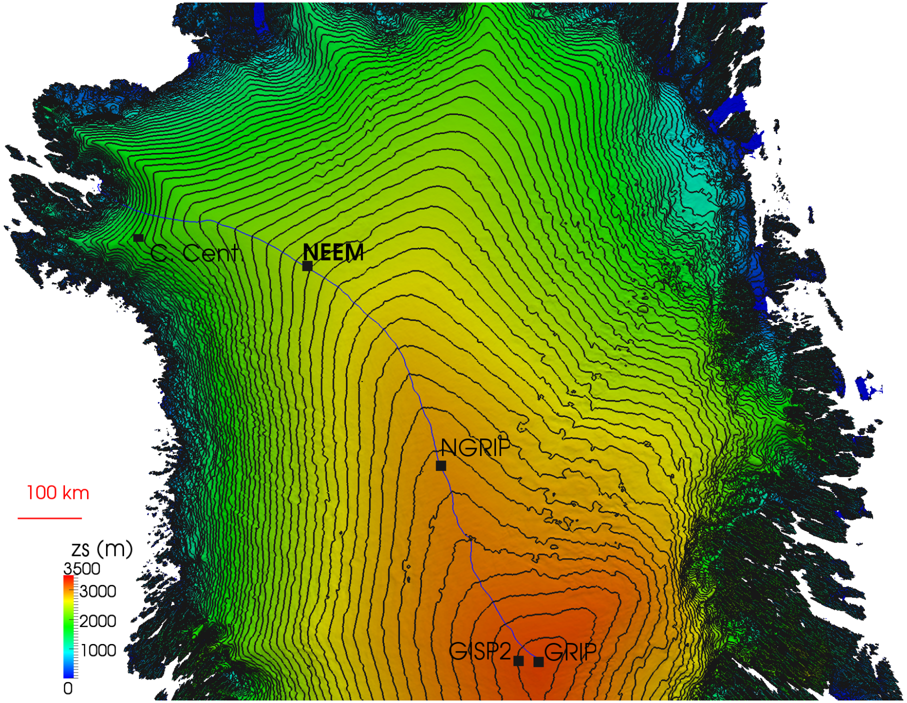

Fig. 1. Greenland Ice Sheet surface elevation (Bamber et al., 2013) and location of the GRIP, GISP2, NorthGRIP, NEEM and Camp Century drilling sites. Contours are every 50 m. A flow line following the greatest slope along the NNW ridge is shown in blue.

TCD
8, 307–335, 2014

Fabric measurement along the NEEM ice core, Greenland

M. Montagnat et al.

Title Page
Abstract | Introduction
Conclusions | References
Tables | Figures
◂ | ▸
Back | Close
Full Screen / Esc
Printer-friendly Version
Interactive Discussion

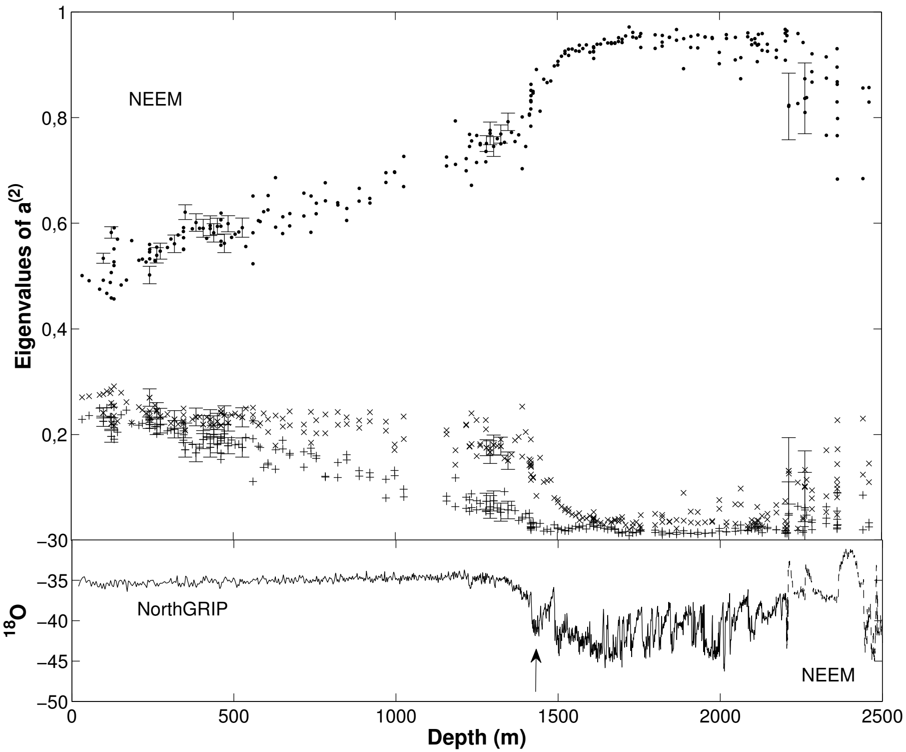

Fig. 2. Top: fabric profile along the NEEM ice core, represented by the eigenvalues of the orientation tensor $\mathbf{a}^{(2)}$. Error bars correspond to a $\pm 1\sigma$ confidence interval (see text). Bottom: evolution of the climate proxy isotope $\delta^{18}O$ from the NorthGRIP ice core transferred to the NEEM depth scale (Rasmussen et al., 2013) for the upper 2200 m, and from the NEEM ice core below 2200 m depth (dashed line) (Dahl-Jensen et al., 2013). The NEEM isotope data are not available yet, but the overall features are very similar to those of NorthGRIP. The arrow represents the depth of the glacial termination at NEEM, 1419 m.

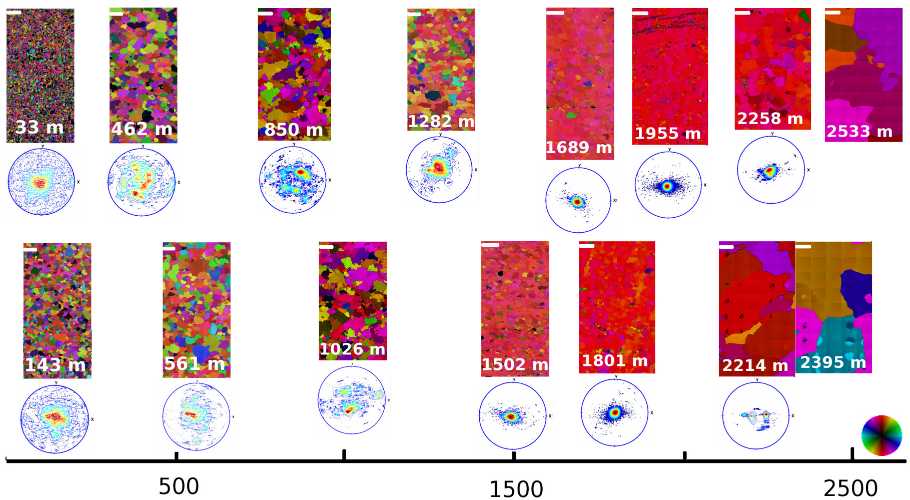

Fig. 3. Evolution with depth of the microstructures observed in *c*-axis orientation color scale (see color wheel on the bottom right), and of the fabric represented by pole figures. The thin sections of dimension about 8 cm × 11 cm are vertical (i.e. in the coring direction). Length scale (white line) is 10 mm. The pole figures are represented with the vertical axis (core axis) perpendicular to plane of the figure.

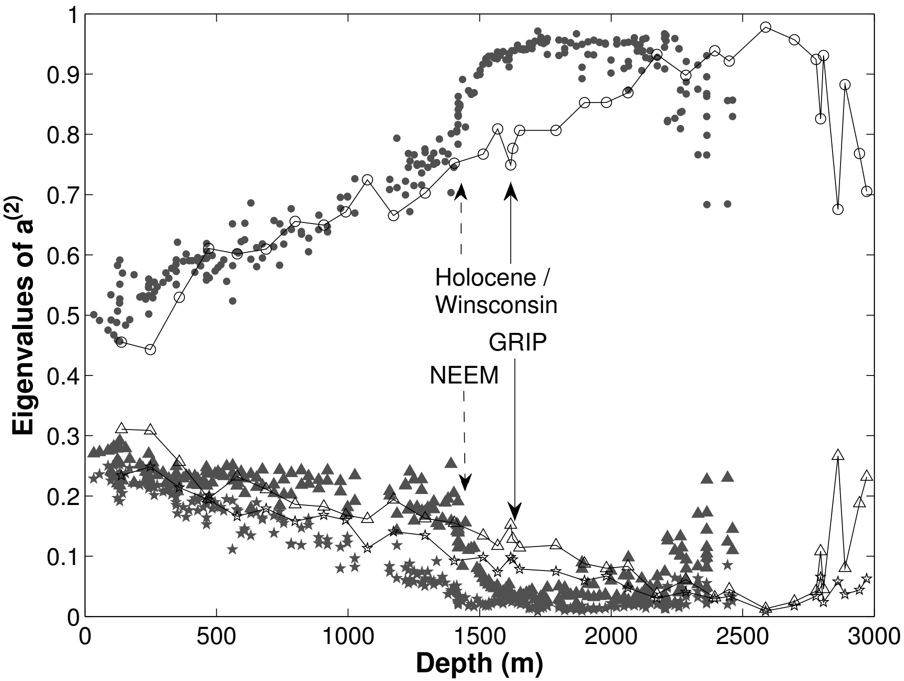

Fig. 4. Comparison between the fabric profiles along the NEEM ice core (filled symbols) and the GRIP ice core (open symbols) (Thorsteinsson et al., 1997; Svensson et al., 2009).

TCD
8, 307–335, 2014

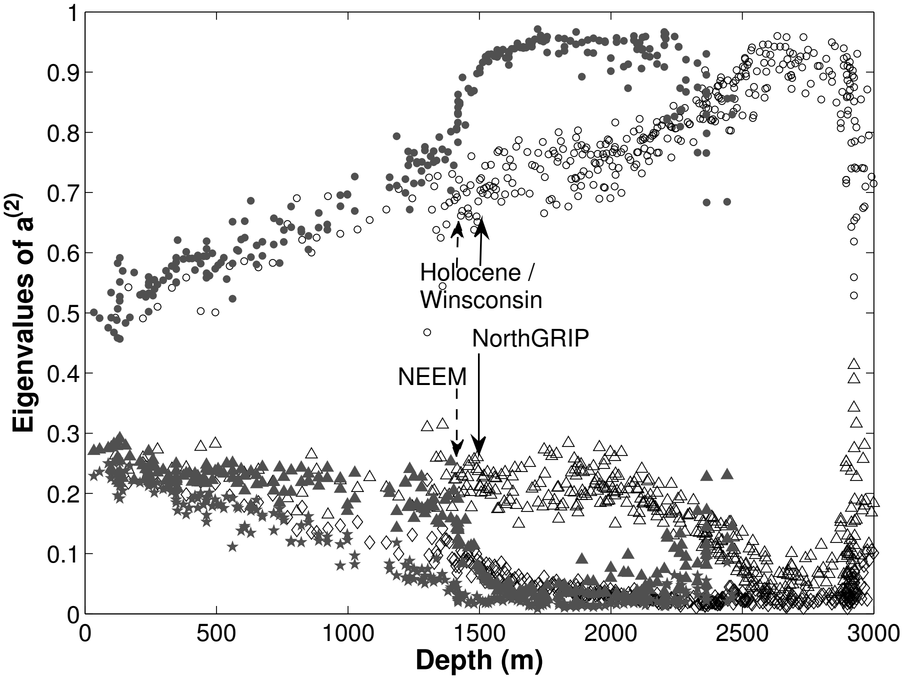

Fig. 5. Comparison between the fabric profiles along the NEEM ice core (filled symbols) and the NorthGRIP ice core (open symbols) (Wang et al., 2002; Svensson et al., 2009).

TCD
8, 307–335, 2014

Fabric measurement along the NEEM ice core, Greenland

M. Montagnat et al.

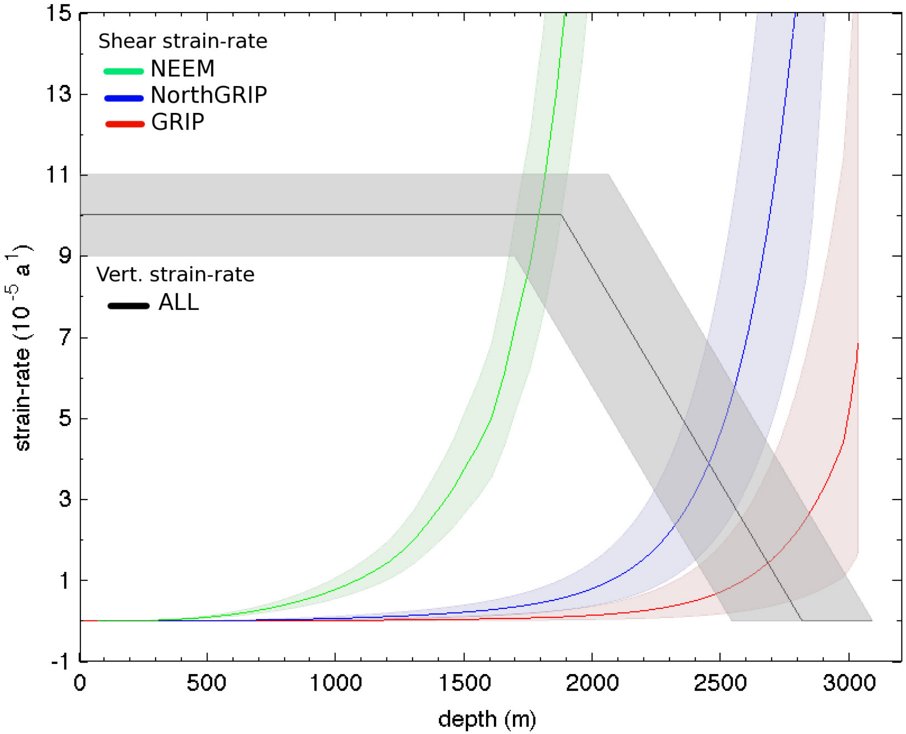

Fig. 6. Evolution of the shear strain-rates, D_{xz}, along the GRIP (red), NorthGRIP (blue) and NEEM (green) ice cores with error bars. The black line represents the estimated evolution of the vertical strain-rate D_{zz}, which is basically the same for all three cores regarding the error bars.

TCD
8, 307–335, 2014

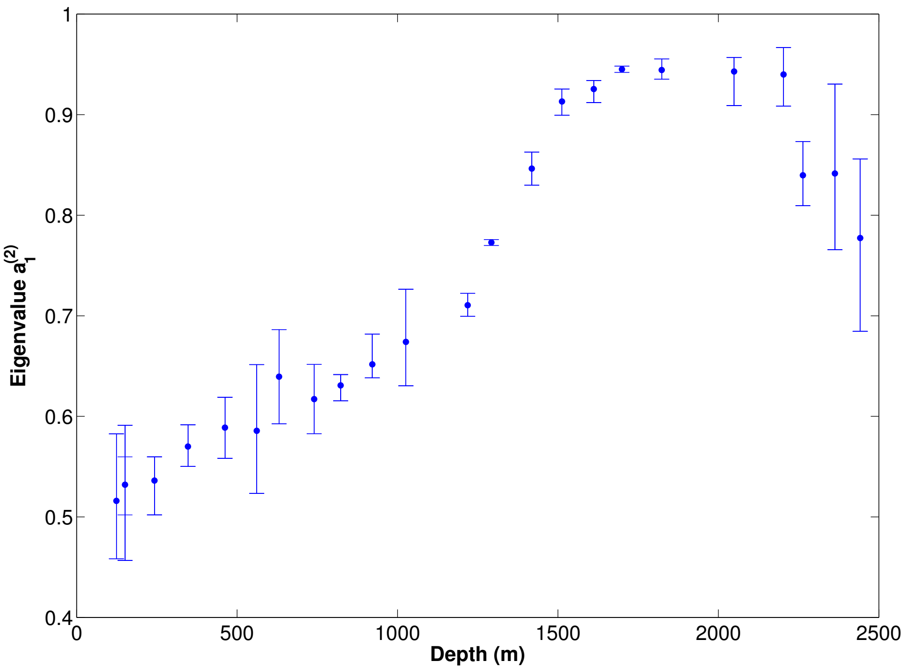

Fig. 7. Variability of the fabric eigenvalue $a_1^{(2)}$ measured along the NEEM ice core. Each point represents the average fabric measured along 55 cm core by contiguous thin sections. The given depth (x-axis) is the depth of the upper part of the 55 cm core. The vertical bars extend from the minimum to the maximum value measured around the mean.

TCD
8, 307–335, 2014

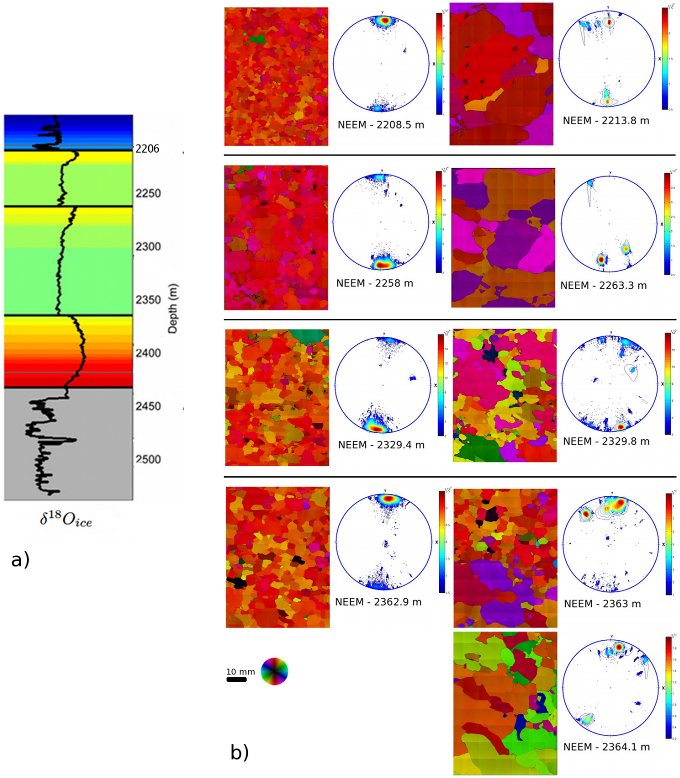

Fig. 8. Abrupt variations of fabrics and microstructures around the discontinuities observed in the $\delta^{18}O_{ice}$ signal **(a)** (Dahl-Jensen et al., 2013). Different colors along the stable isotope record highlight the disturbed sections. The reconstructed age-scale corresponds to a continuous color scale. Microstructure and fabric data **(b)** were chosen on each side of the various discontinuities, but also to reveal other discontinuities (see text). The length scale is the same for all microstructure images (black line). The orientation color scale is given by the color wheel. The pole figures are plotted with the vertical axis (core axis) vertical in the plane of the figure.

TCD
8, 307–335, 2014